Available online at www.sciencedirect.com

ScienceDirect

Procedia Structural Integrity 18 (2019) 205–213

Structural Integrity Procedia

www.elsevier.com/locate/procedia

25th International Conference on Fracture and Structural Integrity

Influence of temperature on fracture toughness values in different regions of A-387 Gr. B welded joint

Ivica Čamagić[a], Simon A. Sedmak[b,*], Aleksandar Sedmak[c], Zijah Burzić[d]

[a]*Faculty of Technical Sciences, 7 Kneza Miloša Street, K. Mitrovica, Serbia*
[b]*Innovation Center of the Faculty of Mechanical Engineering, 16 Kraljice Marije Street, Belgrade, Serbia*
[c]*Faculty of Mechanical Engineering, 16 Kraljice Marije Street, Belgrade, Serbia*
[d]*Military Institute of Techniques, 1 Ratka Resanovića Street, Belgrade, Serbia*

Abstract

The influence of temperature on fracture toughness values in different regions of a welded joint is analysed low-alloyed Cr-Mo steel A-387 Gr. B, designed for high temperature applications. Heterogeneity of microstructure and properties of welded joint is evaluated by testing standard 3BP specimens with crack tip located at different regions of a joint, including the base metal (BM), weld metal (WM) and heat-affected-zone (HAZ). Experiments were performed both at the room temperature and at design working temperature, 540□C. Based on these results, temperature effect on crack resistance is established for all different regions in a welded joint.

Peer-review under responsibility of the Gruppo Italiano Frattura (IGF) ExCo.

Keywords: : low-alloyed steel; welded joint; crack; plane strain fracture toughness, critical crack length.

1. Introduction

By analysing the brittle behaviour of bodies with cracks, fracture mechanics provided new possibilities for ensuring welded joint safety. Standard ASTM E399 [1] for determining of fracture toughness under plain strain, $K_{Ic,}$ completes the process of linear elastic fracture mechanics application to real structures, made of high strength materials, wherein presence of cracks results in plane strain state. The main condition for the validity of such tests is that the plastic strain is only present in a negligible area around the crack tip, prior to crack propagation and fracture. Since for most

* Corresponding author.
E-mail address: simon.sedmak@yahoo.com

2452-3216
Peer-review under responsibility of the Gruppo Italiano Frattura (IGF) ExCo.
10.1016/j.prostr.2019.08.155

structural materials and welded joints, the plastic strain area around the crack tip is large, direct determining of the K_{Ic} parameter is not possible, and its application to real conditions is limited.

Parent material (PM) testing, as well as testing of welded joint components (weld metal – WM and heat affected zone - HAZ) of a low-alloyed steel involved the determining of fracture mechanics parameters of the PM and welded joint components, at room temperature and at an elevated temperature of 540°C, [2].

2. Materials for testing

The parent material was steel A-387 Gr. B with thickness of 102 mm. Chemical composition and mechanical properties of the PM are given in tables 1 and 2, [2, 3].

Table 1. Chemical composition of PM specimens

Specimen mark	% mas.							
	C	Si	Mn	P	S	Cr	Mo	Cu
N	0,13	0,23	0,46	0,009	0,006	0,85	0,51	0,035

Table 2. Mechanical properties of PM specimens

Specimen mark	Yield stress, $R_{p0,2}$, MPa	Tensile strength, R_m, MPa	Elongation, A, %	Impact energy, J
N	325	495	35,0	165

Welding of steel sheets made of this parent material was performed in two stages, according to the requirements given in the welding procedure provided by a welding specialist, and these stages include:

- Root weld by E procedure, using a coated LINCOLN S1 19G electrode (AWS: E8018-B2), and
- Filling by submerged arc welding (SAW), wherein wire denoted as LINCOLN LNS 150 and powder denoted as LINCOLN P230 were used as additional materials.

Chemical composition of the coated electrode LINCOLN S1 19G, and the wire LINCOLN LNS 150 is given in tab. 3, whereas their mechanical properties are given in tab. 4, [2, 3].

Table 3. Chemical composition of additional welding materials

Filler material	% mas.						
	C	Si	Mn	P	S	Cr	Mo
LINCOLN Sl 19G	0,07	0,31	0,62	0,009	0,010	1,17	0,54
LINCOLN LNS 150	0,10	0,14	0,71	0,010	0,010	1,12	0,48

Table 4. Mechanical properties of additional materials

Additional material	Yield stress, $R_{p0,2}$, MPa	Tensile strength, R_m, MPa	Elongation, A, %	Impact energy, J at 20°C
LINCOLN Sl 19G	515	610	20	> 60
LINCOLN LNS 150	495	605	21	> 80

Butt welded joint was made with a U-weld. The shape of the groove for welding preparation was chosen based on thickness, in accordance with appropriate standards SRPS EN ISO 9692-1:2012, [4], and SRPS EN ISO 9692-2:2008, [5].

3. Determination of plane strain fracture toughness, K_{Ic}

The influence of temperature on the parent material and welded joint components tendency towards brittle fracture was assessed by determining fracture toughness in plain strain conditions, i.e. by determining the critical value of

stress intensity factor, K_{Ic}. Tests were performed at room temperature of 20°C, as well as at the elevated temperature of 540°C.

For the purpose of determining K_{Ic}, three point bending specimens (SEB) were used for room temperature testing, and their geometry was defined in accordance with standards ASTM E399 [1] and ASTM E1820, [6]. For determining K_{Ic} at the temperature of 540°C, modified CT specimens, whose geometry was defined in accordance with standard BS 7448 Part 1 [7], were used.

Fracture toughness, K_{Ic}, determined directly using critical J-integral, J_{Ic}, by using elastic-plastic fracture mechanics (EPFM), as defined by standards ASTM E813 [8], ASTM E 1737 [9], ASTM E1820 [6] and BS 7448 Parts 1 and 2, [7,10], i.e. by monitoring crack propagation under plastic conditions.

American Society for Testing and Materials (ASTM) defined a standard procedure for obtaining of resistance curves for metallic materials according to crack propagation [8]. The European Structural Integrity Society (ESIS) then worked on improving of this standard [11]. Some of the solutions suggested by this standard were accepted, and in this paper they are related to determining of a fitted regression line. Standards [1,6,8,9,12-14] are updated regularly and thus it is important to use only the most recent versions.

Experiments were performed by testing a single specimen via successive partial unloading, i.e. by single specimen yield method, as defined by standard E813 [8]. The goal of the yield method is to register the magnitude of crack propagation, Δa, which occurred during the test, after unloading. The testing itself was performed with specimens which had fatigue cracks in PM, WM and HAZ, at room temperature of 20°C and the elevated temperature of 540°C, using an electric mechanical tensile test machine.

In the case of room temperature testing, the specimens was equipped with a COD extensometer for the purpose of measuring crack tip opening. This was not the case when testing was performed at elevated temperatures. Namely, due to the lack of extensometer that can work at these temperatures, crack tip opening was registered using an inductive sensor, with previously registered calibration curve, showing the ratio between values obtained using the extensometer and those obtained from the sensor.

Bending or tensile load (depending on the type of specimen being tested) was applied at a slow rate, 1 mm/min. The load was applied with periodic unloading, up to a point where considerable plastic strain started occuring or the specimen fractured, i.e. once the extensometer /inductive sensor range was exceeded. During this time, an A/D converter was used

Based on the yield, which represents the ratio between force increment and crack tip opening increment on the unloading line, it is possible to determine crack length using the following expression:

$$\Delta a_i = \Delta a_{i-1} + \left(\frac{b_{i-1}}{\eta_{i-1}}\right) \cdot \left(\frac{C_i - C_{i-1}}{C_{i-1}}\right) \tag{1}$$

where:

a_{i-1} – previous crack length;

$C_i = tg\alpha_i$ – slope of the observed unload line;

$C_{i-1} = tg\alpha_{i-1}$ – slope of the previous unload line;

$\eta_{i-1} = 2$ –SEB specimen coefficient; $\eta_{i-1} = 2 + 0{,}522\, b_i/W$ – CG specimen coefficient;

W – specimen width and

b_{i-1} – previous ligament length.

J-integral is equal to the sum of its elastic and plastic components [15]:

$$J_{(i)} = J_{el} + J_{pl} \tag{2}$$

For SEB and CT specimens, the elastic J-integral component, i.e. the elastic energy component, is calculated based on the expression [15]:

$$J_{el(i)} = \frac{K_i^2 \cdot \left(1 - \nu^2\right)}{E} \tag{3}$$

where:

K_i – stress intensity factor, defined according to standard ASTM E 399;

v - Poisson's ratio and
E – Elasticity module.
Stress intensity factor Ki for SEB specimens is calculated using the following expression:

$$K_i = \frac{F_i \cdot S}{(B \cdot B_N)^{1/2} \cdot W^{3/2}} \cdot f(a_0/W) \tag{4}$$

whereas for CT specimens:

$$K_i = \frac{F_i}{(B \cdot B_N \cdot W)^{1/2}} \cdot f(a_i/W) \tag{5}$$

The geometry term f(a0/W), in the case of SEB specimens, is determined as:

$$f(a_0/W) = \frac{3(a_0/W)^{1/2}\left[\begin{array}{l}1{,}99 - (a_0/W)(1 - a_0/W)\cdot \\ \cdot\left(2{,}15 - 3{,}93(a_0/W) + 2{,}7(a_0/W)^2\right)\end{array}\right]}{2(1 + 2\,a_0/W)(1 - a_0/W)^{3/2}} \tag{6}$$

and for CT specimens:

$$f(a_i/W) = \frac{(2 + a_i/W)\left[\begin{array}{l}0{,}866 + 4{,}64(a_i/W) - 13{,}32(a_i/W)^2 + \\ + 14{,}72(a_i/W)^3 - 5{,}6(a_i/W)^4\end{array}\right]}{(1 - a_i/W)^{3/2}} \tag{7}$$

Plastic component of the J-integral is calculated based on the following expression [15]:

$$J_{pl(i)} = \left[J_{pl(i-1)} + \left(\frac{\eta_i}{b_i}\right)\frac{A_{pl(i)} - A_{pl(i-1)}}{B_N}\right] \cdot \left[1 - \gamma_i \frac{(a_i - a_{i-1})}{b_i}\right] \tag{8}$$

where:
B – specimen thickness;
a_0 – initial fatigue crack length;
A_{pl} – plastic energy component;
S – span between the supports;
B_N – specimen net width;
$\eta_i = 2$ – SEB specimen coefficient; $\eta_i = 2 + 0{,}522\ b_i/W$ – CT specimen coefficient;
$\gamma_i = 1$- for SEB specimens and
$\gamma_i = 1 + 0{,}76\ b_i/W$ – for CT specimens.

Based on the obtained data, a J-Δa curve is drawn, and the regression line is then constructed on it, according to standard ASTM E1152 [13]. Critical value of J-integral, J_{Ic}, is then obtained from this regression line. By knowing the values of J_{Ic}, it is possible to calculate the critical stress intensity factor (fracture toughness), K_{Ic}, for plane strain, using the following relation:

$$K_{Ic} = \sqrt{\frac{J_{Ic} \cdot E}{1 - \nu^2}} \tag{9}$$

Calculated values of critical stress intensity factor are given in table 5, for specimens with the notch in the PM, tested at room temperature and at the elevated temperature of 540°C, [15]. It is important to note that the calculation of fracture toughness for plane strain used different elasticity module values for room temperature (210 GPa) and for elevated temperature (cca 160 GPa for 540°C).

Typical F-δ and J-Δa diagrams for specimens taken out of the parent material, tested at room temperature and the elevated temperature of 540°C are not shown here, due to the scope of this paper [15]. The influence of test temperature

on critical stress intensity factor values, for PM specimens is graphically represented in fig. 1, whereas its influence on critical crack length, a_c, is shown in fig. 2, [15].

Table 5. Values of K_{Ic} notched specimens in PM

Specimen mark	Testing temperature, °C	Critical J-integral, J_{Ic}, kJ/m^2	Critical stress intensity factor, K_{Ic}, MPa m$^{1/2}$	Critical crack length, a_c, mm
PM-1-1n		60,1	117,8	38,5
PM-1-2n	20	63,9	121,4	40,8
PM-1-3n		58,6	116,3	37,5
PM-2-1n		43,2	87,2	40,0
PM-2-2n	540	44,7	88,7	41,4
PM-2-3n		45,3	89,2	41,9

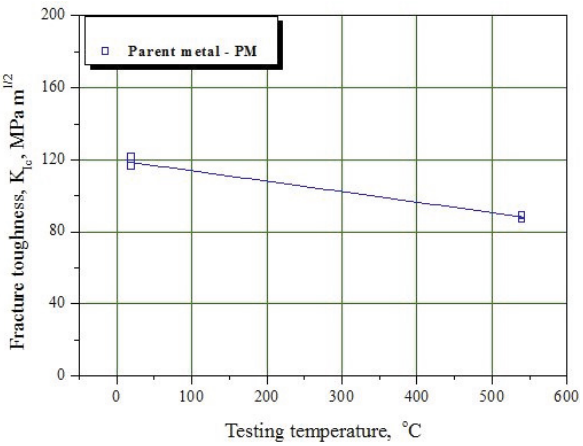

Figure 1. Change in value of $_{KIc}$, depending on the testing temperature for PM specimens

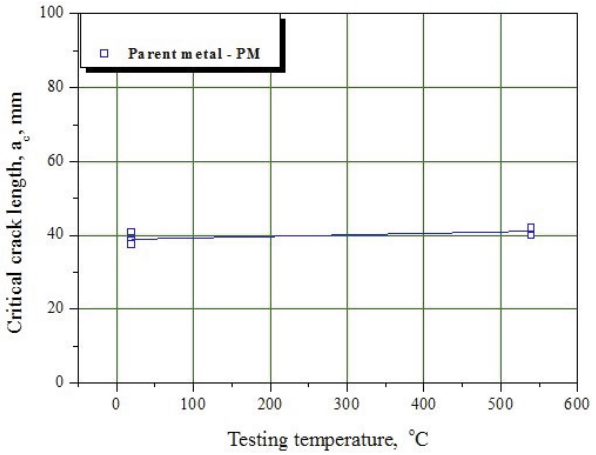

Figure 2. Change in value of a_c, depending on the testing temperature for PM specimens

Calculated value of critical stress intensity factor, K_{Ic}, and critical crack length, ac, are given in table 6, for specimens with the notch in the WM, tested at both room and elevated temperatures [15].

Table 6. Values of, K_{Ic} notched specimens at WM

Specimen mark	Testing temperature, °C	Critical J-integral, J_{Ic}, kJ/m^2	Critical stress intensity factor, K_{Ic}, MPa m$^{1/2}$	Critical crack length, a_c, mm
WM-1-1		72,8	129,6	20,2
WM-1-2	20	74,3	130,9	20,7
WM-1-3		71,1	128,1	19,8
WM-2-1		50,2	93,9	17,4
WM-2-2	540	52,6	96,2	18,2
WM-2-3		48,4	92,2	16,8

F-δ and *J-Δa* diagrams for the specimen with a notch in the WM are shown in fig. 3, for specimen denoted as WM-1-1, tested at room temperature, and in fig. 4, for specimen denoted as WM-2-1, tested at 540°C.

The effect of test temperature on critical stress intensity factor values for specimens with the notch in the WM is shown graphically in fig. 5, whereas the effect of test temperature on critical crack length values, ac, is shown in fig. 6, [15]. Calculated value of critical stress intensity factor, K_{Ic}, and critical crack length, ac, are given in table 7, for specimens with the notch in the HAZ, tested at both room and elevated temperatures [15].

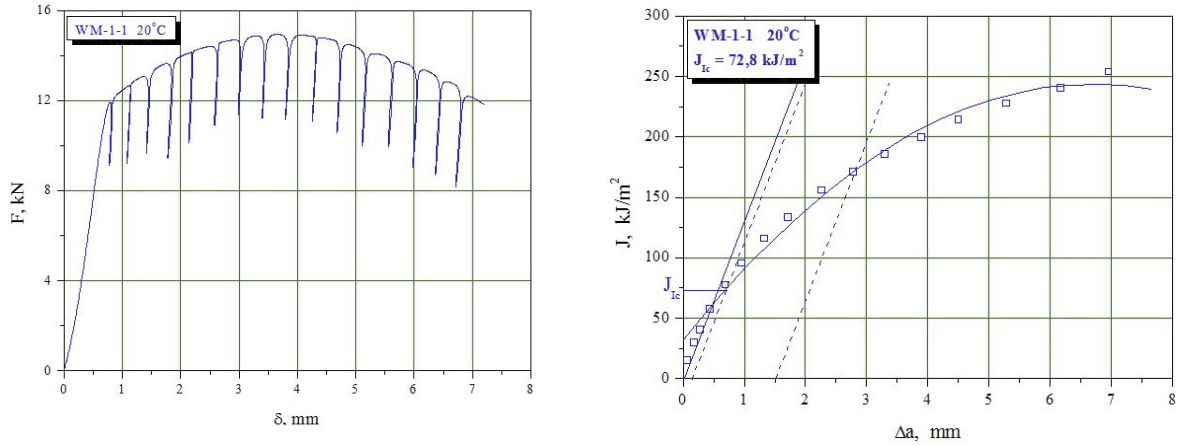

Figure 3. *F-δ* (left) and *J-Δa* (right) diagrams for specimen WM-1-1

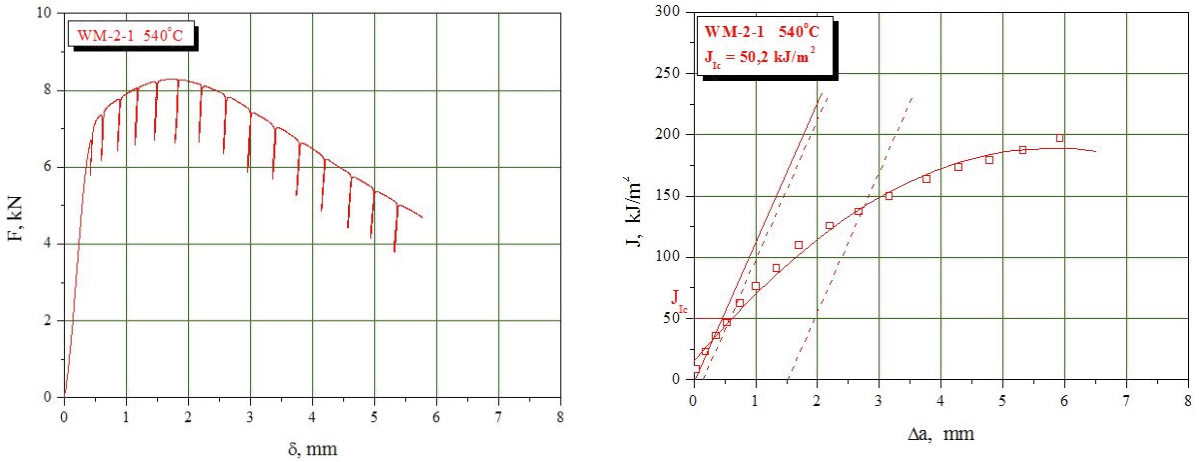

Figure 4. *F-δ* (left) and *J-Δa* (right) diagrams for specimen WM-2-1

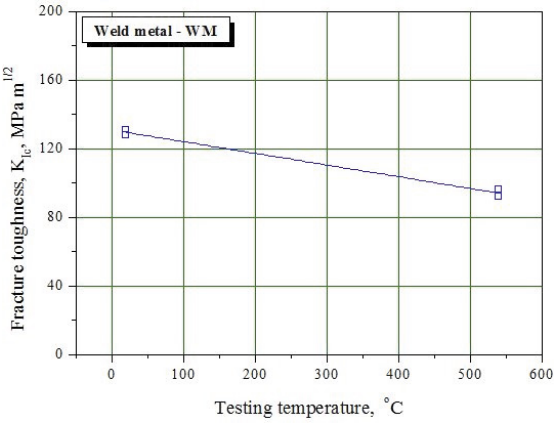

Figure 5. Change in value of K_{Ic}, depending on the testing temperature for WM specimens

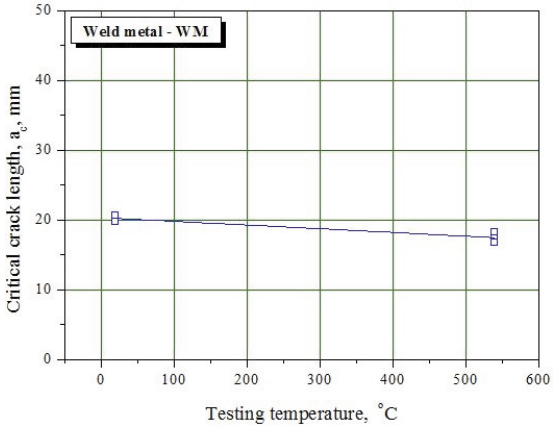

Figure 6. Change in value of a_c, depending on the testing temperature for WM specimens

Typical *F*-δ and *J*-Δa diagrams for specimens taken from the HAZ, tested at room and elevated temperatures, are not shown here, due to the scope of this paper [15]. The effect of test temperature on critical stress intensity factor values for specimens with the notch in the HAZ is shown graphically in fig. 7, whereas the effect of test temperature on critical crack length values, a_c, is shown in fig. 8, [15].

Table 7. Values of, KIc notched specimens at HAZ

Specimen mark	Testing temperature, °C	Critical J-integral, J_{Ic}, kJ/m^2	Critical stress intensity factor, K_{Ic}, MPa m$^{1/2}$	Critical crack length, a_c, mm
HAZ-1-1n		53,6	111,2	34,3
HAZ-1-2n	20	51,7	109,2	33,0
HAZ-1-3n		49,8	107,2	31,8
HAZ-2-1n		33,6	76,9	31,1
HAZ-2-2n	540	34,2	77,5	31,6
HAZ-2-3n		36,1	79,7	33,4

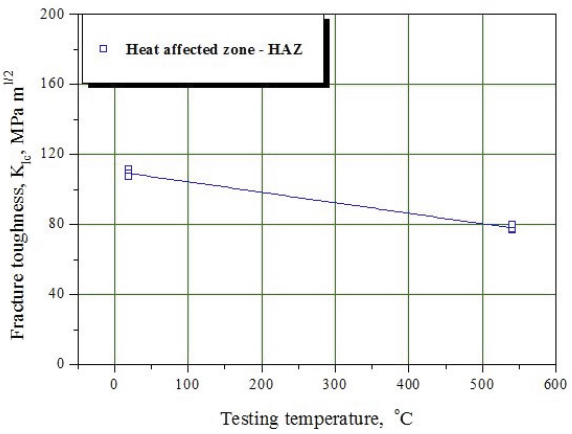

Figure 7. Change in value of K_{Ic}, depending on the testing temperature for HAZ specimens

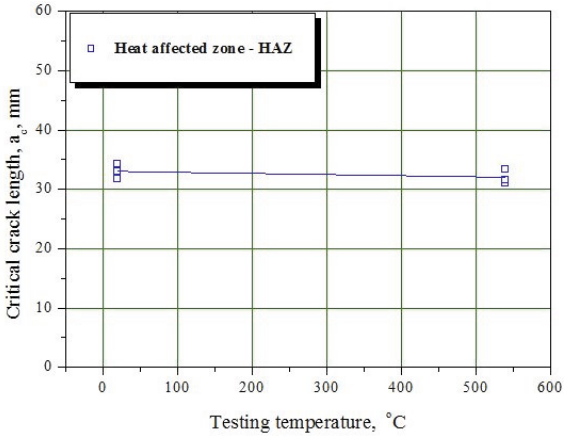

Figure 8. Change in value of a_c, depending on the testing temperature for HAZ specimens

4. Discussion

Based on the results obtained by testing of specimens taken out of the PM, it can be seen that the increase in test temperature leads to decreased critical J-integral values, hence fracture toughness, K_{Ic} also decreases.

Fracture toughness values for PM specimens, shown in tab. 5, range from 118 MPa m$^{1/2}$ at room temperature to 88 MPa m$^{1/2}$ at 540°C [15].

Obtained critical crack length, a_c, values in the case of the PM did not show noticeable changes with temperature. This was expected since critical crack length was calculated using real yield stress values, obtained from tensile tests [16].

Based on the results obtained by testing of specimens with the notch in the WM, it can be seen that the increase in test temperature leads to decreased critical J-integral values, hence fracture toughness, K_{Ic} also decreases. Fracture toughness values for these specimens, given in tab. 6, range from 130 MPa m$^{1/2}$ at room temperature, to 94 MPa m$^{1/2}$ at 540°C [15].

Obtained critical crack length, a_c, values, are significantly lower relative to yield stress level, ranging from 20.2 mm at room temperature to 17.5 mm at 540°C. However, if critical crack length values are calculated based on the PM yield stress, they are considerably higher, suggesting high brittle fracture resistance of the WM [16].

Based on the results obtained by testing of specimens taken out of the HAZ, it can be seen that the increase in test temperature leads to decreased critical J-integral values, hence fracture toughness, K_{Ic} also decreases. The same can be concluded for critical crack length, a_c.

Fracture toughness values for HAZ specimens, shown in tab. 7, range from 109 MPa $m^{1/2}$ at room temperature, to 78 MPa $m^{1/2}$ at 540°C, [15]. Obtained critical crack length values do not change significantly with the temperature, for HAZ specimens [15].

5. Conclusion

Weakest resistance towards crack growth under static force, i.e. lowest K_{Ic} values were measured for specimens with the notch in the HAZ, whereas highest resistance was measured in the case of specimens with the notch in the WM. The change in the slope of the curves is caused by changes in test temperature, notch location and exploitation duration. By analysing the obtained curves, it can be seen that the individual curves in each groups exhibit almost identical dependence from the above mentioned factors, with differences in maximum force values, F_{max}, which is directly related to fatigue crack length [15].

Results obtained from fracture mechanics parameters (K_{Ic}, J_{Ic}, and a_c) indicated that the tendency toward brittle fracture under static loading is lowest in the case of specimens with cracks in the WM and the PM, whereas it was highest for specimens with a crack in the HAZ, i.e. HAZ specimens had lowest resistance toward brittle fracture in this case.

6. Acknowledgements

Parts of this research were supported by the Ministry of Sciences and Technology of Republic of Serbia through Mathematical Institute SANU Belgrade Grant OI 174001 Dynamics of hybrid systems with complex structures. Mechanics of materials and Faculty of Technical Sciences University of Pristina, residing in Kosovska Mitrovica.

References

[1] ASTM E399-89, Standard Test Method for Plane-Strain Fracture Toughness of Metallic Materials, Annual Book of ASTM Standards, Vol. 03.01. p. 522. 1986.

[2] Ivica Camagic, Simon A. Sedmak, Aleksandar Sedmak, Zijah Burzic, Mihajlo Arandjelovic, The impact of the temperature and exploitation time on the tensile properties and plain strain fracture toughness, KIc in characteristic areas of welded joint, Frattura ed Integrita Strutturale, ISSN 1971-8993, No. 46, Vol. 12, (October 2018), pp. 371-382, DOI: 10.3221/IGF-ESIS.46.34, GRUPPO ITALIANO FRATTURA, VIA G DI BIASIO, CASSINO, ITALY, 03043, https://www.fracturae.com/index.php/fis/issue/view/299.

[3] Ivica Čamagić, Simon Sedmak, Aleksandar Sedmak, Zijah Burzić, Aleksandar Todić, Impact of Temperature and Exploitation Time on Plane Strain Fracture Toughness, KIc, in a Welded Joint, STRUCTURAL INTEGRITY AND LIFE, ISSN 1451-3749) (printed edition), EISSN 1820-7863 (Online), Vol. 17, No. 3, 2017, pp. 239–244, http://divk.inovacionicentar.rs/ivk/ivk17/239-IVK3-2017-IC-SAS-AS-ZB-AT.pdf.

[4] SRPS EN ISO 9692-1:2012, Welding and allied processes - Recommendations for joint preparation - Part 1: Manual metal-arc welding, gas-shielded metal-arc welding, gas welding, TIG welding and beam welding of steels (ISO 9692-1:2003), 2012.

[5] SRPS EN ISO 9692-2:2008, Welding and allied processes - Joint preparation - Part 2: Submerged arc welding of steels (ISO 9692-2:1998), 2008.

[6] ASTM E 1820-99a, Standard Test Method for Measurement of Fracture Toughness, Annual Book of ASTM Standards, Vol. 03.01, 1999.

[7] BS 7448-Part 1, Fracture mechanics toughness tests-Method for determination of K_{Ic} critical CTOD and critical J values of metallic materials, BSI, 1991.

[8] ASTM E813-89, Standard Test Method for J_{Ic}, A Measure of Fracture Toughness, Annual Book of ASTM Standards, Vol. 03.01. p. 651, 1993.

[9] ASTM E 1737-96, Standard Test Method for J Integral Characterization of Fracture Toughness, Annual Book of ASTM Standards, Vol.03.01., 1996.

[10] BS 7448-Part 2, Fracture mechanics toughness tests - Methods for determination of K_{Ic}, critical CTOD and critical J values of welds in metallic materials, BBI, 1997.

[11] "ESIS Procedure for Determining the Fracture Behavior of Materials", European Structural Integrity Society ESIS P2-92, 1992.

[12] BS 5762-DD 19, Standard Test Method for Crack Opening Displacement, London, 1976.

[13] ASTM E1152-91, Standard Test Method for Determining J-R Curve, Annual Book of ASTM Standards, Vol. 03.01. p. 724, 1995.

[14] ASTM E 1290-89, Standard Test Method for Crack-Tip Opening Displacement (CTOD) Fracture Toughness Measurement, Annual Book of ASTM Standards, Vol. 03.01, 1993.

[15] Ivica Čamagić, Investigation of the effects of exploitation conditions on the structural life and integrity assessment of pressure vessels for high

temperatures (in Serbian), doctoral thesis, Faculty of Technical Sciences, Kosovska Mitrovica, 2013
[16] I. Camagic, Z. Burzic, A. Sedmak, H. Dascau, L. Milovic, Temperature effect on a low-alloyed steel welded joints tensile properties, The 3rd IIW South – East European Welding Congress, "Welding & Joining Technologies for a Sustainable Development & Environment", June 3-5, 2015, Timisoara, Romania, Proceedings (77-81), ISBN 978-606-554-955-5.